Rev. Adv. Mater. Sci. 28 (2011) 48-53

EFFECT OF CARBIDE TYPE ON THE MANUFACTURING AND PROPERTIES OF LOW VACUUM PLASMA SPRAYED W-BASED COMPOSITE COATING MATERIAL

Young-Min Jin[1], Jin-Hyeon Cho[1], Jee-Hoon Ahn[2] and Kee-Ahn Lee[1]

[1]School of Advanced Materials Engineering, Andong National University, Andong 760-749, Korea
[2]Hybrid Materials Processing Research Department, RIST, Pohang, 790-330, Korea

Received: February 17, 2011

Abstract. Two types of W-based composite powders containing ZrC or HfC were prepared by PAS method and the manufacturing of W-based composite coating was attempted by using LVPS deposition process. The macroscopic coating properties, high-temperature ablation resistance, adhesive strength, and microstructural observation of the LVPS W composite coatings were also investigated.

1. INTRODUCTION

Compared to the properties of other thermal resistant materials, tungsten normally has a much higher melting point (3683K), as well as outstanding thermal and mechanical shock resistance, and resistance to high temperature. Such properties of the tungsten have been drawing attention to its potential as appropriate thermal materials for airplane parts, automobile engines, rocket engine nozzles, *etc*. The superior thermal properties of tungsten are known to be improved by combining carbides (ZrC, HfC, TiC) or elements such as Re as tungsten-based composites. Most tungsten-alloys have been usually manufactured in bulk via HIP (hot isostatic pressing) or sintering process. Related research has been reported on the changes in the high-temperature mechanical and ablation properties [1,2]. However, production of tungsten composite materials via the above-mentioned processes has its limits in being applied to complex configurations and large-area parts.

VPS (vacuum plasma spray) is a process wherein superior thermal materials are melted at high-temperatures in a high speed thermal plasma jet and sprayed to the surface of parts inside a sealed vacuum chamber. On the application of VPS and other coating processes for ultra-high thermal materials, X. Liu *et al.* [3] used a plasma spray method to produce a pure tungsten coating layer, while D. J. Varaclle *et al.* [4] attempted to create a pure ZrC coating by using VPS. Despite the attempts, the majority of studies on W-based coatings reported so far deal with changes made to the microstructure following the manufacturing of the coating layer and those made to basic physical properties. Relatively few studies have been reported on the production of coatings for different types of carbide or on related properties.

This study attempted to produce a tungsten-based composite coating layer via LVPS, by using tungsten-based composite powders that were manufactured by adding different types of carbide with a PAS. Effect of carbide type on the macroscopic coating properties (high temperature ablation resistance, hardness, bond strength, and microstructure) was also investigated, and the mecha-

Corresponding author: Kee-Ahn Lee, e-mail: keeahn@andong.ac.kr

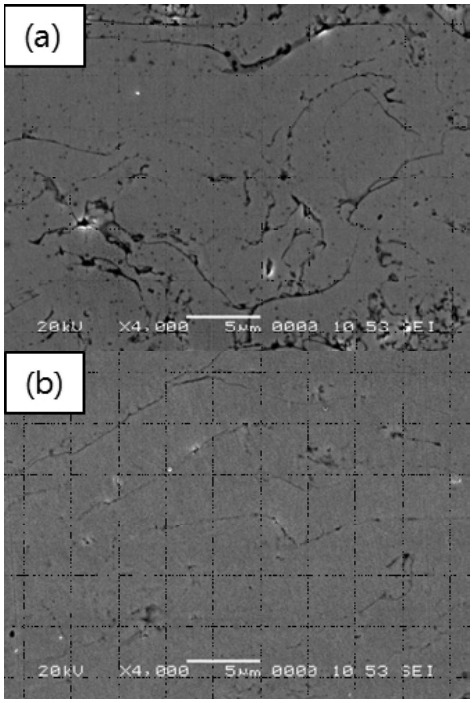

Fig. 1. Cross-sectional images of LVPS coating layers using (a) SD&S powders and (b) PAS powders.

nism of the ultra high thermal resistance of W-HfC and W-ZrC coating layers was discussed.

2. EXPERIMENTAL METHODS

Tungsten-based composite powders (W-HfC, W-ZrC: 4-6%) were manufactured by using PAS (Plasma Alloying and Spheroidization) process from the raw powders of pure tungsten, 99.5% HfC, and 99.5% ZrC. During PAS, powder feedstock is fed into a plasma stream where melting occurs and surface tension causes spherical droplets to be formed [5]. To determine if the PAS-manufactured powder is more appropriate for preparing a coating layer than powder manufactured via conventional SD&S (spray drying & sintering), pre-experiment was conducted using tungsten powder. Tungsten PAS powder represented the tap density of 11.74 g/cm^3, which is superior to the 3.62 g/cm^3 density of the tungsten SD&S powder. Fig. 1 shows the cross-sectional micrographs of the tungsten coating layers produced by pre-experiment. The results show that the coating layer via PAS power-based LVPS has a denser structure and lower porosity than the coating layer via SDS. Fig. 2 shows the configurations and particle size distributions of manufactured W-based composite powders. Regardless of type and particle size, both W-HfC and W-ZrC powders have a spherical shape. The average particle sizes of powders were 29.76 μm (W-HfC) and 27.58 μm (W-ZrC), respectively. LVPS (low vacuum plasma spray) process was used to manufacture W-HfC and W-ZrC composite coatings on the substrate of graphite. A pre-experiment was carried out to obtain optimal process conditions. Thus, 120 SLPM Ar flow rate, 12 SLPM H_2 flow rate, 1490 A current, 350 mm spray distance, 50 mbar

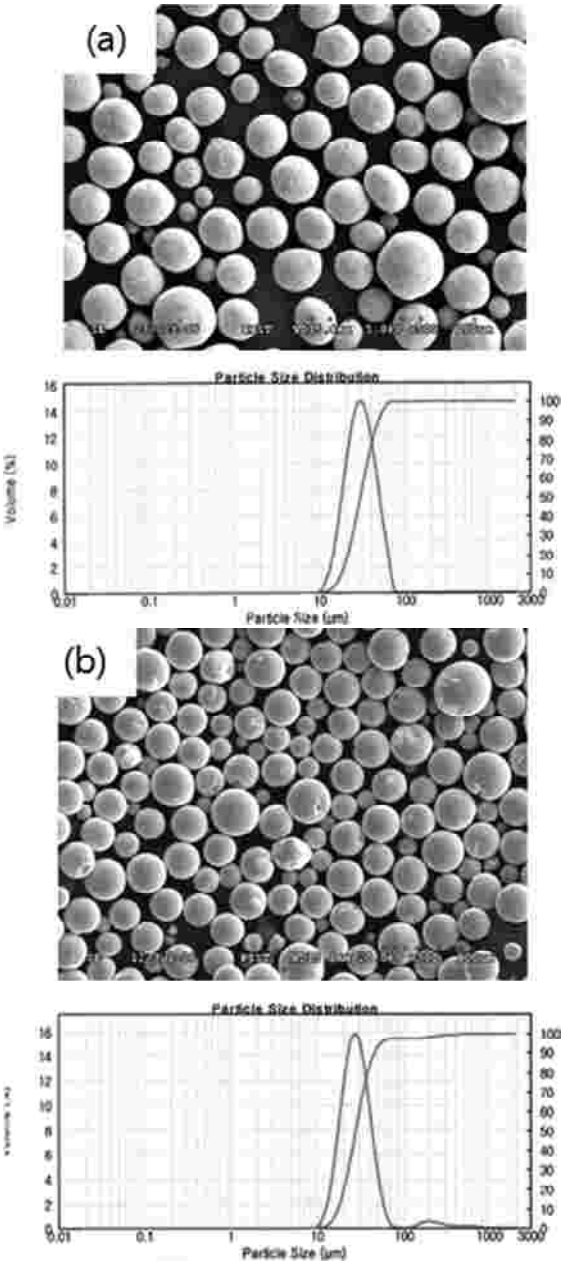

Fig. 2. SEM images and the size distributions of (a) W-HfC and (b) W-ZrC composite powders.

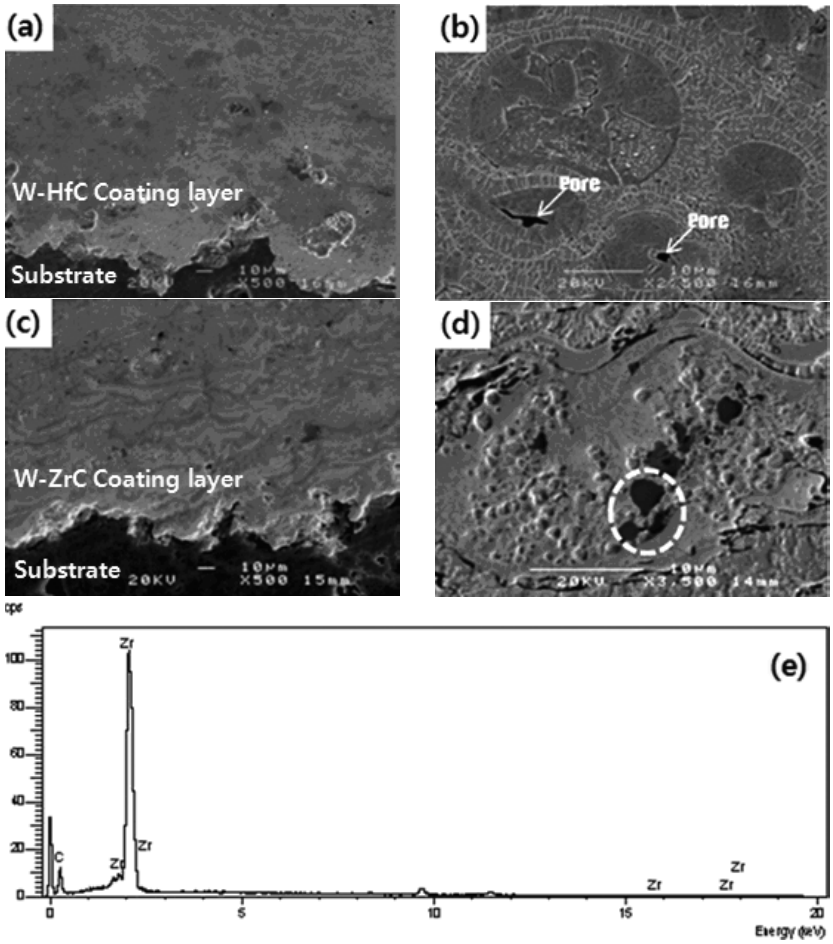

Fig. 3. SEM micrographs of W-HfC coating layer (a), (b), that of W-ZrC coating layer (c), (d), and (e) EDS analysis result of dark gray phase (dashed circle in (d)) in W-Zr coating layer.

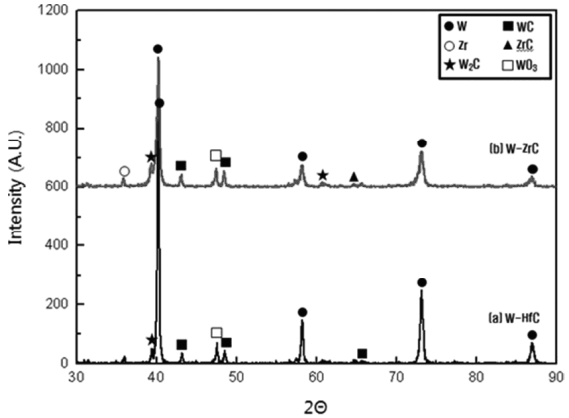

Fig. 4. XRD analysis results of (a) W-HfC and (b) W-ZrC coating layers.

vacuum, and 1200 °C substrate preheating conditions were used in this study for the manufacturing of W-HfC and W-ZrC coating layers. Image analyzer was used to measure porosity. Vickers hardness measurement also conducted under loading of 10 g. Measuring of the adhesive strength of the coatings layer was carried out under crosshead speed of 1 mm/min in accordance with the ASTM C 633. Evaluation of the ultrahigh thermal-resistant properties of W-based composite coating layers was conducted via plasma torch test at approximately 12,000~16,000 °C and for 20-50 seconds. After the test, weight loss of the specimens was measured to compare the high-temperature ablation-resistant properties with time. XRD, SEM, optical micrographs were also used to observe microstructure and to identify phases.

3. RESULTS AND DISCUSSION

The composite coating layers via LVPS were produced using two different types of W-carbide composite powders, each approximately 1000 μm in thickness. Fig. 3 shows SEM micrographs of W-HfC and W-ZrC coating layers. Basically, both layers showed the lamellar splat which is the typical

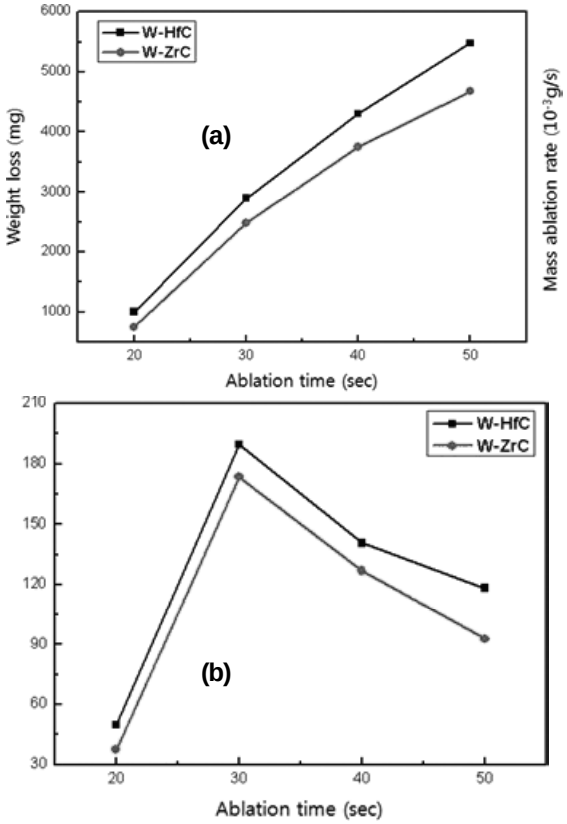

Fig. 5. Plasma torch test results of W-HfC and W-ZrC composite coating layers, based on (a) weight loss, and (b) mass ablation loss rate.

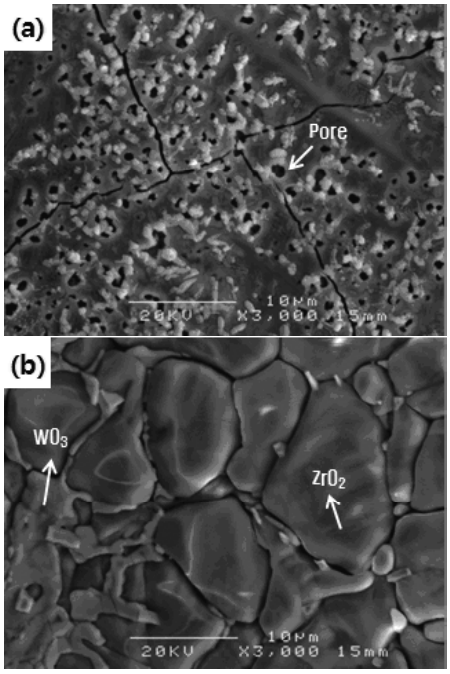

Fig. 6. SEM images of the surfaces of plasma torch tested (a) W-HfC and (b) W-ZrC coating layers.

structure of LVPS coatings, double-layered columnar structure and pores inside the splat. In the EDS analysis results, both W-HfC and W-ZrC had a tungsten matrix and the W-ZrC coating layer represented partial distribution of the dark gray phase(dashed circle in (d)), where a relatively higher level of Zr and C contents ((e)) were found unlike the W-HfC coating (near-zero distribution of HfC).

Fig. 4 shows the results of the XRD in the LVPS W-based coating layers. Both layers showed the creation of W, WC, W_2C, and WO_3 phases. As inferred from results of the microstructure and EDS (Fig. 3), the W-HfC layer did not show the Hf or HfC peak, whereas the W-ZrC layer revealed minimal peaks of both Zr and ZrC. It could be assumed that all HfC particles were melted into the tungsten matrix during the LVPS process, whereas some portions of non-melted ZrC particles remained in the W-ZrC layer.

According to the results of porosity measurement, W-HfC had a ratio of 3.59%, a lower value than that of W-ZrC, i.e., 7.74%. Hardness values of these two W-based coating layers were 867.06 Hv (W-HfC) and 984.51 Hv (W-ZrC), respectively. Despite its nearly two-fold porosity, the W-ZrC coating had a hardness approximately 120 Hv higher than that of the W-HfC. The difference is assumed to be attributed to the partial reinforcement effects of ZrC particles that remain in the W-ZrC composite coating layer. Adhesive strength of the W-HfC composite coating layer was 41.1 kgf/cm^2 and that of the W-ZrC was 38.3 kgf/cm^2, representing similar adhesive strengths.

Fig. 5 shows the results of plasma torch test conducted on the W-based coating layers, in terms of accumulated weight loss (Fig. 5a) and mass ablation rate (Fig. 5b) with time. After the testing of 50 seconds, the W-HfC and W-ZrC coating layers each lost weight of 5484 mg and 4890 mg, respectively. The results (Fig. 5) indicate that the W-ZrC coating has a somewhat higher level of high temperature ablation resistance than the W-HfC coating. In Fig. 5b, it is noted that the mass ablation loss rate increases rapidly in the initial stage (up to 30 seconds), then decreases with increasing exposure time regardless of containing carbide type. Chen *et al.* [6] suggested in carbon composite material that the increase of the ablation loss rate at the initial stage is closely related to abrupt exposure of material itself to the high temperature environment. And

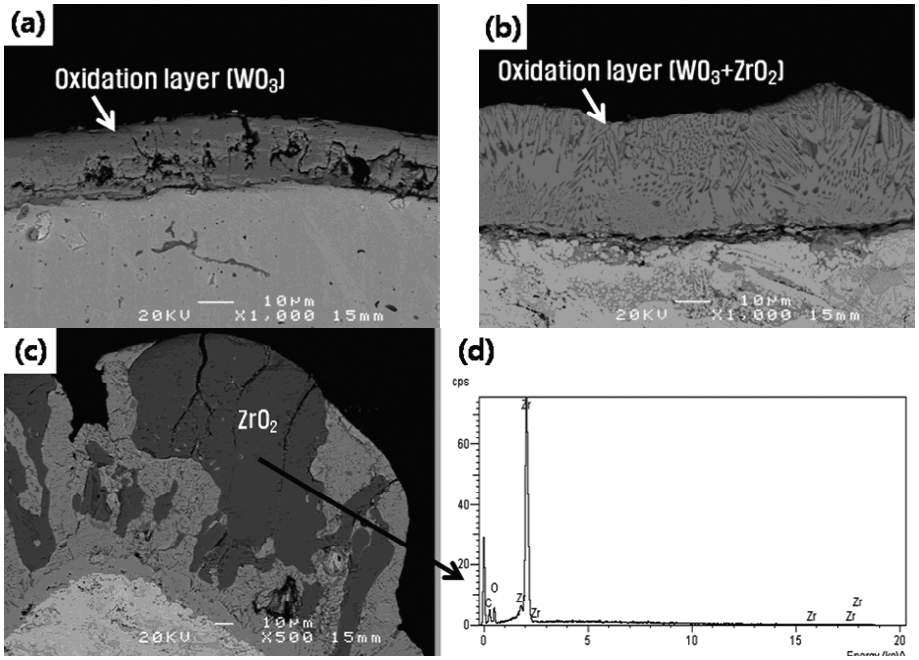

Fig. 7. Cross-sectional image of plasma torch tested W-HfC (a), of W-ZrC (b) and (c) layers, and of EDS analysis of dark gray phase in the W-ZrC oxidation layer (d).

then, the decrease of the mass loss rate is mainly due to the formation of reaction oxides on the surface during test [6]. It could be understandable that the W-ZrC coating layer represented a lower-level of mass ablation rate at the early stage than the W-HfC did as some of the ZrC particles remaining in the W-ZrC layer acted as a reinforcing phase. And then, the W-ZrC layer's lower ablation rate (negative slope) at the later stages of the test was presumably due to the interaction between the new oxide phases formed on the surface and the high-temperature environment.

Some cracks could be observed on the surface of W-HfC coating layer after the testing (Fig. 6a), due to thermal shock. In addition, micro-sized pores were observed that had been formed amidst the discharge of gases generated by the oxidation of the coated layer. Also, reaction oxides of irregular shapes were observed on the layer's surface after the testing. In contrast, no such micro-sized pores were found on the surface of W-ZrC composite coating (Fig. 6b). And the reaction products created on the surface of the layer took the form of consistent masses in the W-ZrC coating layer.

Fig. 7 illustrates cross-sectional micrographs of W-HfC and W-ZrC coating layers after plasma torch test. Both layers show the oxidation layers formed on the surface of each of the layers. A thicker and denser oxidation layer was found in the W-ZrC (Fig. 7b) than in the W-HfC (Fig. 7a). In the microstructures observation and XRD results, WO_3 (W-HfC coating), WO_3 and ZrO_2 (W-ZrC coating) phases were each confirmed in each of the coated layers. It should also be noted that no damage was inflicted upon the interior coating layers after the plasma torch test. This indicates that the oxidation layers (WO_3 and ZrO_2) formed on the W-HfC and W-ZrC coating layers during the torch test effectively protect the inner coating layers against the high temperature ablation environment. It is also assumed that the oxide layer can hinder the heat transfer and the diffusion of oxidative gas in the W-based composite coating material. Nevertheless, based on the previously-obtained results of the accumulated weight loss and mass ablation rates of the specimens (Fig. 5), it can be inferred that the additional ZrO_2 (melting point of 2677 °C) oxide formed on the W-ZrC coating layer was more effective than the WO_3 (1470 °C) in improving high-temperature thermal and ablation resistance.

4. CONCLUSIONS

The LVPS coatings of W-HfC and W-ZrC composite powders (PAS) successfully led to the production of two coating layers, each measuring about 1,000 μm in thickness. W-ZrC coating layer showed a partial presence of ZrC particles that were not

completely melted. Porosity results showed that the W-HfC coating layer had a lower ratio than the W-ZrC layer. The higher hardness of W-ZrC layer than that of W-HfC layer, is presumably due to the reinforcing effects of ZrC particles. Microstructural observation for the specimens after plasma torch test showed that a new oxidation layer was formed on the surface of the coating layer. The new layer consisted of WO_3 (W-HfC), WO_3 and ZrO_2 (W-ZrC). Even after the testing, the inner layers of coating remained nearly intact, indicating superior thermal resistance. According to the results of ultra high-temperature thermal resistance test, the W-ZrC layer showed superior high-temperature thermal resistance. It is thought to be attributed to the reinforcement effects of ZrC during the earlier stage (up to 30 seconds) and the protective effects of ZrO_2, the new phase developed on the surface of the W-ZrC layer, at the later stage of the test.

REFERENCES

[1] A. Luo, K.S. Shin and D.L. Jacobson // *Acta metal. Mater.* **9** (1992) 2225.
[2] G.M. Song, Y. Zhou and Y.J. Wang // *Mater. Charact*. **50** (2003) 293.
[3] X. Liu, S. Tamura *et al.* // *J. Nuclear Mater*. **329** (2004) 687.
[4] D.J. Varacalle Jr., L.B. Lundberg *et al.* // *Surf. Coat. Technol.* **68** (1994) 86.
[5] J.S. O'Dell, E.C. Schofield, T.N. McKechnie and A. Fulmer // *J. Mater. & Perfor*. **13** (2004) 461.
[6] C.Z. Ke, X. Xiang, L.G. Dong and W.Y. Lei // *Applied Surf. Sci*. **255** (2009) 9217.